Biosensors and Bioelectronics 72 (2015) 148–155

Contents lists available at ScienceDirect

Biosensors and Bioelectronics

journal homepage: www.elsevier.com/locate/bios

Silicon/SU8 multi-electrode micro-needle for *in vivo* neurochemical monitoring

Natalia Vasylieva [a,b], Stéphane Marinesco [b], Daniel Barbier [a], Andrei Sabac [a,*]

[a] Lyon Institute of Nanotechnologies, CNRS UMR 5270, INSA de Lyon, 7, avenue Jean Capelle, 69621 Villeurbanne Cedex, France
[b] INSERM U1028, CNRS UMR 5292, Lyon Neuroscience Research Center, Team WAKING, 8 avenue Rockefeller, University Claude Bernard Lyon 1, 69373 Lyon Cedex 08, France

ARTICLE INFO

Article history:
Received 3 April 2015
Accepted 5 May 2015
Available online 6 May 2015

Keywords:
bioMEMS
Microfabrication
Glucose
Lactate
Rat brain
Enzymatic biosensor

ABSTRACT

Simultaneous monitoring of glucose and lactate is an important challenge for understanding brain energetics in physiological or pathological states. We demonstrate here a versatile method based on a minimally invasive single implantation in the rat brain. A silicon/SU8-polymer multi-sensing needle-shaped biosensor, was fabricated and tested. The multi-electrode array design comprises three platinum planar microelectrodes with a surface area of $40 \times 200\ \mu m^2$ and a spacing of 200 μm, which were micromachined on a single 3 mm long micro-needle having a $100 \times 50\ \mu m^2$ cross-section for reduced tissue damage during implantation. Platinum micro-electrodes were aligned at the bottom of micro-wells obtained by photolithography on a SU8 photoresist layer. After clean room processing, each micro-electrode was functionalized inside the micro-wells by means of a micro-dispensing device, either with glucose oxidase or with lactate oxidase, which were cross-linked on the platinum electrodes. The third electrode covered with Bovine Serum Albumin (BSA) was used for the control of non-specific currents. The thick SU8 photoresist layer has revealed excellent electrical insulation of the micro-electrodes and between interconnection lines, and ensured a precise localization and packaging of the sensing enzymes on platinum micro-electrodes. During *in vitro* calibration with concentrations of analytes in the mM range, the micro-wells patterned in the SU8 photoresist proved to be highly effective in eliminating cross-talk signals, caused by H_2O_2 diffusion from closely spaced micro-electrodes. Moreover, our biosensor was successfully assayed in the rat cortex for simultaneous monitoring of both glucose and lactate during insulin and glucose administration.

1. Introduction

Detecting biomolecules in the central nervous system and monitoring their concentration over time is an important goal in neuroscience and human medicine. For example, comatose patients treated after severe hemorragic stroke or traumatic brain injury, are often equipped with intracerebral probes to monitor the extracellular brain concentrations of glucose, lactate and pyruvate. Such probes help reveal possible neurological complications and direct neurological treatment (Bellander et al., 2004). In animals, glucose and lactate monitoring is an important challenge to understand brain energetics in physiological or pathological states.

Implantable microelectrode biosensors provide an attractive strategy for brain metabolites monitoring. Typically, an oxidaze enzyme layer that selectively recognizes the molecule of interest covers the platinum microelectrode. and degrades a substrate of interest while producing hydrogen peroxide (H_2O_2), which is detected on the surface of microelectrode (Dale et al., 2005). A screening layer coating the electrodes prevents the oxidation of endogenous electroactive molecules present in the brain such as serotonin, dopamine, ascorbate, and cysteine etc. (Bruno et al., 2006; Dale et al., 2005; Frey et al., 2010; Pernot et al., 2008; Wassum et al., 2008). Each electrode can be coated with only one enzyme, and therefore can only detect one molecule. For achieving parallel monitoring of several molecules, single wire-based multiplex probes will produce several penetrations raising the risk of brain injury. As a whole, there is a need for miniaturized biosensor probes allowing single penetration to achieve parallel monitoring of different analytes.

The interest for biocompatible, less invasive sensors has motivated research on new materials and architectures (Hajj-Hassan et al., 2008; Kotzar et al., 2002; Navarro et al., 2005). While many planar multi-electrode sensors have been developed for *in vivo* brain implantation and for the detection of local field potentials or neuronal unitary activity (Buzsáki, 2004; Kipke et al., 2008), chemical sensing of endogenous molecules present in the interstitial

* Corresponding author. Fax: +33 472438531.
E-mail address: andrei.sabac@insa-lyon.fr (A. Sabac).

http://dx.doi.org/10.1016/j.bios.2015.05.004
0956-5663/

fluid of the brain is less developed.

Planar multi-electrode biosensors have been developed for *in vivo* neurochemical monitoring on ceramic substrate (Bruno et al., 2006; Burmeister et al., 2000; Rutherford et al., 2007; Wassum et al., 2008), on silicon substrate (Frey et al., 2010; Ruther et al., 2008; Wassum et al., 2012, 2008) and recently on polyimide substrate (Weltin et al., 2014). Silicon, widely employed in Micro-Electro-Mechanical-Systems (MEMS) offers strength and elasticity necessary for construction of bioprobes. These attributes subsequently increase safe and reliable *in vivo* implantation. Silicon can also be processed by different well developed MEMS-technologies that are not easily adaptable for ceramic supports or bulk polymer materials. For example, silicon wafers can be selectively etched to define the dimensions of the final needle, while ceramic probes possess a fixed thickness, usually of some hundreds of micrometers that yields thicker devices (Burmeister and Gerhardt, 2003) and possible more extensive tissue damage.

Most of the reported planar devices allowed monitoring of only one analyte with half of the microelectrodes devoted to enzymatic sensing and the other half devoted to the control of non-specific currents (Rutherford et al., 2007; Wassum et al., 2008; Weltin et al., 2014). A few reports demonstrated successful parallel recordings of choline and acetylcholine (Burmeister et al., 2008) or glutamate and non-specific (control) current (Frey et al., 2010) using multi-sensing micro-arrays without significant cross-talk between recording sites. These probes were used for detection of analytes present in low concentrations *in vivo* but not for glucose and lactate that reach mM concentrations *in vivo*, thereby increasing the risk of electrochemical cross-talk.

Cross-talk depends on the distance between adjacent electrodes and on the concentration of H_2O_2 diffusing out of the enzyme layer to distant recording sites which is proportional to the concentration of the enzyme substrate in the solution. Less cross-talk occurs for molecules present in low μM concentration which is usually the case for glutamate, choline, and D-serine, but not for glucose or lactate present *in vivo* at mM concentrations. This problem has been discussed in several studies mainly addressing flow-type integrated sensor probes (Moser, 2002; Palmisano et al., 2000; Quinto et al., 2001; Suzuki and Akaguma, 2000). Using a needle-type multi-sensing microelectrode array Quinto et al. (2001) demonstrated that a non-specific signal representing about 25% of the total oxidation current was detected on an electrode separated by 125 μm from another one modified with glucose oxidase. Suzuki and Akaguma (2000) studied the effects of enzymatic activity as well as membrane density and thickness, on the degree of cross-talk between electrodes. They concluded that more cross-talk was observed in dense and thick enzyme layers when most of the H_2O_2 was produced at the surface of the enzyme-immobilized membrane. These results suggest that cross-talk could be decreased in biosensors prepared with thinner and well localized enzyme layers. Cross-talk can also be reduced by locating each microelectrode at the bottom of micro-well cavities wherein enzymes are deposited. Such micro-wells were demonstrated using anisotropic etching of silicon (Frey et al., 2010).

In this work, we created microwells using the SU8 photoresist, a highly cross-linked epoxy material that can be processed in thick uniform layers. SU8 micro-structures are directly patternable by photolithography yielding high aspect ratio and smooth walls. We designed a three-electrode silicon microneedle with SU8-microwells, and prepared glucose and lactate biosensors that were validated by *in vitro* analyte measurements and *in vivo* parallel monitoring using a single penetration in the rat brain.

2. Material and methods

2.1. Design of the three-electrode implantable micro-needles

Fig. 1A depicts the architecture of our needle-shaped silicon/SU8 multi-sensor with three platinum electrodes centered in SU8 micro-wells onto the silicon tip. Micro-probe was designed to facilitate manipulation and precise insertion in the brain tissue with minimal damage and sufficient stiffness. Our design includes an implantable part consisting of a 3 mm long micro-needle with $100 \times 50\ \mu m^2$ cross-section bearing three platinum electrodes of $40 \times 200\ \mu m^2$ located 300 μm away from the needle tip and with 200 μm spacing between them. An intermediate (non-implantable) 3 mm part of $1000 \times 50\ \mu m^2$ cross-section was defined between the implantable microneedle and the bulk silicon. The control electrode is placed between the lactate and glucose sensing electrodes. The SU8 micro-wells allow the confinement of proteins and limit the diffusion of H_2O_2 between electrodes. The SU8 layer also ensures electrical insulation for the platinum buried contact lines driving the current flow from the electrodes to the conductive pads of the external connector.

2.2. Materials and micro-fabrication of the three-electrode silicon micro-needles

Micro-fabrication sequence of micro-needles is summarized in Fig. 2. Probes were fabricated starting from 4 in., double side polished, 250 μm thick silicon ⟨100⟩ wafers with 400 nm thermally grown oxide. Starting from topside of the wafer, the microelectrodes were patterned by the lift-off technique: e-beam Physical Vapor Deposition (PVD) of 20 nm thick titanium adhesion layer and a subsequent 100 nm thick platinum layer (Fig. 2A). The insulation layer and the micro-wells were patterned by photolithography on SU8-2 (Microchem) negative photoresist. To obtain 4 μm deep micro-wells the photoresist was processed according to manufacturer's directions. Using a mask aligner (EVG 620), microwells patterns were precisely located (< 2 μm) on top of the platinum electrodes. Development was performed in propylene glycol methyl ether acetate (PGMEA) releasing the SU8 microwells and SiO_2 unprotected areas (Fig. 2B). Prior to the silicon microneedle release, a 4 μm protective layer of thick positive photoresist has been deposited by spin coating. Micro-needle edges and back side membrane were aligned to the platinum electrodes and patterned by photolithography (Fig. 2C). This photoresist layer protected the SU8 layer and the electrodes during SiO_2 etching with buffered HF (hydrofluoric acid) and Deep Reactive Ion Etching (DRIE) of the silicon substrate. Deep trenches of 65 μm were achieved by DRIE on the topside in order to form the micro-needle (Fig. 2D). DRIE of the backside membrane (Fig. 2E) completes the release of the micro-needle (Fig. 2F). The electrical contacts were soldered with ultrasonic assistance to a commercial circuit board and afterwards insulated with UV epoxy glue.

2.3. Microelectrode treatment

Prior to enzyme immobilization on microelectrodes, the surface was cleaned electrochemically by scanning potential over a range of −1 to 1 V at 100 mV/s *vs.* chloride-treated silver wire (Ag/AgCl) in 1 M H_2SO_4 for 15 times or until stable signal is obtained.

To achieve selective detection *in vivo*, all microelectrodes were coated with a screening layer of electropolymerized poly-m-phenylenediamine (PPD). The PPD screening layer was deposited by electropolymerization for 20 min in 100 mM m-phenylenediamine (Sigma-Aldrich, Saint-Quentin Fallavier, France) solution in 0.01 M PBS at pH 7.4 under a constant potential of +700 mV *vs.* an Ag/AgCl reference electrode. After deposition micro-needles were

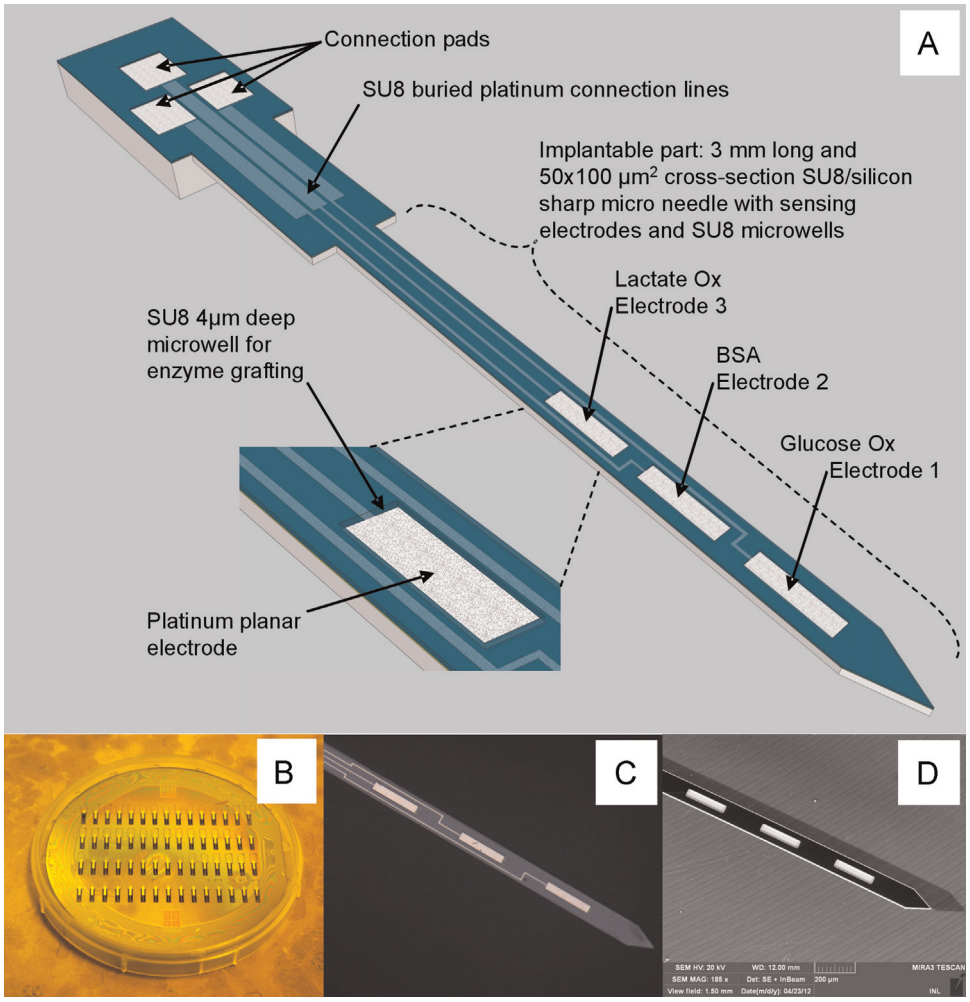

Fig. 1. Silicon/SU8 micro-needle multi-electrode sensor: (A) micro-probe design; (B) image of 4-in. wafer with 60 processed micro-needles; (C) optical image showing electrodes with connection lines and (D) SEM image of the implantable micro-needle and three electrodes surrounded by SU8 micro-wells.

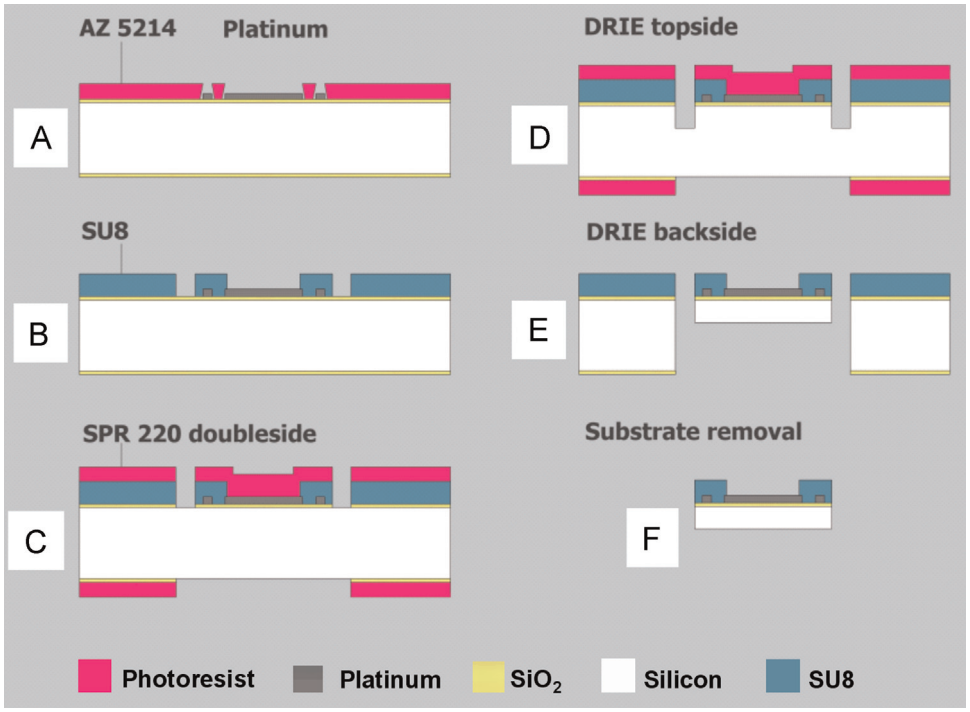

Fig. 2. Main steps in silicon/SU8 multi-electrode micro-needle fabrication (see Section 2.2 for details).

rinsed in DI-water.

2.4. Protein solutions preparation

Bovine Serum Albumin (BSA) solution for the control electrode contained 20 mg/ml BSA and 1% glycerol in Phosphate Buffered Saline solution (PBS 0.01 M, pH 7.4). Glucose oxidase (EC 1.4.3.11) from *Aspergillus niger* (100–250 U/mg) was diluted at 20 mg/mL into a solution of PBS (0.01 M, pH 7.4) containing 20 mg/mL BSA, and 1% glycerol. Lactate oxidase (EC 1.13.12.4) from *Pediococcus sp.* (40 U/mg) was diluted at 20 mg/mL into a PBS solution (0.01 M, pH 7.4) containing 20 mg/mL BSA, 80 mg/mL PEGDE and 0.33% glycerol.

All reagents and enzymes were obtained from Sigma-Aldrich (Saint-Quentin Fallavier, France).

2.5. Enzyme integration

Enzyme solution contained in a glass capillary was dispensed through its tip with opening diameter of less than 40 μm. The other extremity of the capillary is connected through polyethylene tubing to a pneumatic picopump (PV 820, WPI, Hertfordshire, UK) (Fig. 3A). Brief pulses of nitrogen gas with controlled pressure and duration deliver three drops of enzyme solution, with a total volume of about 200 pL directly onto the SU8 micro-wells at the surface of electrodes.

As previously demonstrated (Vasylieva et al., 2013) glucose detection was not affected when the enzyme was immobilized with glutaraldehyde. Therefore we used this method for BSA and glucose oxidase immobilization on the micro-array electrodes because it lasted only 8 min. Lactate oxidase was very sensitive to glutaraldehyde. Immobilization resulted either in complete enzyme deactivation or insufficient fixation. Thus, in our hands poly (ethylene glycol) diglycidyl ether (PEGDE) appeared more suitable for lactate oxidase fixation (Vasylieva et al., 2011). Sensitive and stable biosensors were obtained using solution containing 20 mg/mL of lactate oxidase, 20 mg/mL of BSA and 80 mg/mL of PEGDE in PBS buffer (10 mM, pH 7.4). For electrodes covered with BSA and glucose oxidase the proteins were immobilized by exposure to saturated glutaraldehyde vapors for 8 min. The third electrode was covered with lactate oxidase solution containing the PEGDE cross-linking agent. The immobilization reaction was completed in an oven at 56 °C for 2 h.

To protect the enzymes from bio-fouling in the brain and to widen the linear response range of biosensors a polyurethane membrane was deposited by dip-coating in a 2–3% polyurethane solution in THF (Sigma-Aldrich, Saint-Quentin Fallavier, France) applied in 3–6 dips separated by 10 min at room temperature.

2.6. In vitro calibration

In vitro calibrations were performed in PBS (0.01 M, pH 7.4). The reference electrode Ag/AgCl was placed directly in the recording chamber and constant potential current recordings were obtained at +500 mV optimal for H_2O_2 oxidation, a product of enzymatic reactions (Pernot et al., 2008). Before the experiments, all sensors were tested in serotonin (5-HT, 20 μM in PBS), enzyme substrate (glucose and lactate 10 μM in PBS), and H_2O_2 (1 μM in PBS). Only electrodes with an effective PPD screening layer exhibiting less than 1.2 μA mM^{-1} cm^{-2} response for 5-HT were included in the study, which represented a yield of more than 95% of all electrodes.

2.7. In vivo experiments

All experiments were performed under isoflurane anesthesia, and the animals were treated according to European directive 2010/63/EU. The experimental procedure was validated by the local committee on animals in research of University Claude Bernard Lyon I under reference BH-2010-19. Adult, male Wistar rats weighing 300–500 g were placed in a stereotaxic apparatus (Stoelting, Dublin, Ireland). Their body temperature was maintained at 37 °C. A single needle probe with glucose, lactate and control biosensors was implanted in an area encompassing motor and somatosensory cortices, and avoiding large superficial blood vessels (2–4 mm posterior to bregma, 2–3 mm lateral, 2.5 mm ventral to the dura). Recordings were started at least 1 h after implantation to ensure stabilization of the baseline electrochemical currents. Insulin (25 U/kg of body weight) was injected after an additional 30 min period of control recording, and 1 h later an injection of glucose (3 g/kg of body weight) was administered. Quantitative assessments of brain glucose concentrations were obtained by subtracting the non-specific current of the control biosensor from the output of the glucose and lactate biosensors. The biosensors were calibrated before and after the experiments to ensure that the sensitivity remained stable. If the sensitivity of the biosensor varied by more than 40%, the *in vivo* data were discarded, this represented about 25% of our experiments.

2.8. Amperometric recordings

All recordings were obtained using a VA-10 electrochemistry amplifier (NPI Electronics, Tamm, Germany) equipped with a two-electrode potentiostat. Data acquisition was performed using a 16-bit USB-6221 acquisition board (National Instruments, Nanterre, France) controlled by homemade software based on Igor Pro 6.4 procedures (Wavemetrics, Eugene, OR). The oxidation current

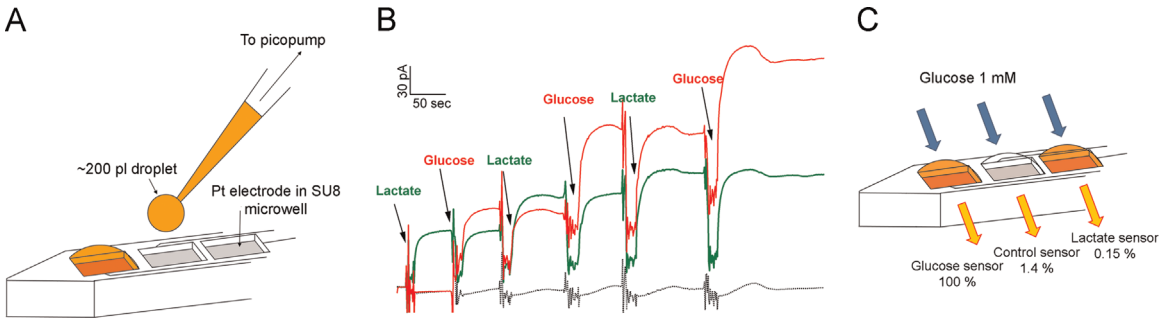

Fig. 3. Enzyme localization and *in vitro* cross-talk characterization. (A) Enzyme dispensing system used to apply enzyme solution over the SU8 micro-well electrode. (B) Alternate injections of glucose and lactate solutions increases the oxidation current on correspondent biosensors of glucose (red) and lactate (green). Control electrode (black) detects non-specific current variations. (C) Cross-talk in the presence of glucose 1 mM was 1.4 ± 1.7% (n=12) on electrode 2, and 0.15 ± 0.19% (n=12) on electrode 3. (For interpretation of the references to color in this figure legend, the reader is referred to the web version of this article.)

was recorded at 1 kHz and averaged over 1000 data points, yielding a final sampling frequency of 1 Hz.

2.9. Data presentation and statistical analyses

Data were presented as mean ± standard deviation. Statistical comparisons between three or more data groups were achieved using an ANOVA followed by Tuckey's post-hoc test.

3. Results and discussion

3.1. Multi-electrode integration on the silicon micro-needle

Our challenge was to perform a parallel and well localized measurement of glucose and lactate, present *in vivo* in the mM range, implying a greater risk of electrochemical cross-talk. The electrodes were placed 200 μm apart, taking into account data published by Quinto et al. (2001). We also adopted a design of micro-wells around electrodes creating a steric barrier for H_2O_2 diffusion out of the well. Although the micro well design had been already proposed in previous works (Frey et al., 2010; Weltin et al., 2014), this is, to our knowledge the first study using only SU8 to create the boundaries between wells. The SU8 resist allowed a large range of possible thicknesses easily achievable by modifying photolithography conditions practical for optimizing the micro-wells design. Additionally, the use of photosensitive resist simplified the overall process allowing a rapid deposition and structuring of the top layer, and avoiding the slow SiO_2 or Si_3N_4 sputtering process or chemical vapor deposition and subsequent dry etch steps.

Implantable multi-electrode probes of 3 mm length and $100 \times 50\ \mu m^2$ cross-section were fabricated with MEMS technology. Fig. 1B shows a picture of successfully processed 4-in. silicon wafer containing 4 rows of 15 silicon/SU8 sharp needles each. SEM micrograph of the final micro-needle revealed a homogeneous SU8 isolation layer without defects or breaks (Fig. 1D). It also revealed the existence of small wells in the SU8 polymer at the bottom of which Pt-electrodes are placed. Fig. 1C depicts the precise alignment of the electrodes and connection lines arrangement on the micro-probe tip.

Each needle therefore possessed three different Pt microelectrodes that were equally sensitive to H_2O_2. Sensitivities for H_2O_2 were 7200 ± 1500, 7200 ± 1000 and 6900 ± 2100 μA mM^{-1} cm^{-2} for electrodes 1, 2 and 3 respectively (n= 6), see (Fig. 1A). For each electrode, the response to H_2O_2 was reproducible: in duplicate H_2O_2 injections, the second response was 99.5 ± 9.1% of the first one (n=24).

3.2. Enzyme immobilization in device and characterization of the multi-biosensor probe

Enzyme solutions have been precisely located by delivering droplets directly onto the electrode SU8-microwells using a home-made dispensing system (Fig. 3A). Fig. 3B demonstrates an *in vitro* glucose and lactate assay of the silicon needle with three electrodes modified by lactate oxidase, BSA and glucose oxidase without the polyurethane diffusive barrier. Injection of lactate (10 μM) leads to a step in the oxidation current on the lactate biosensor (green line), while the currents on the control electrode (BSA, black line) and glucose biosensor (red line) remain unchanged. The subsequent injection of glucose (10 μM) increases oxidation current on the glucose biosensor and not on the control electrode or lactate biosensor thereby, demonstrating parallel independent detection.

We quantified the cross-talk between electrodes as the oxidation current that was measured on electrodes 2 and 3 when glucose was applied to the microneedle (expressed as a percentage of the oxidation current on electrode 1 coated with glucose oxidase, Fig. 3C). Cross-talk was 1.4 ± 1.7% on electrode 2, and 0.15 ± 0.19% on electrode 3 (n=12). Therefore, the level of interference between electrodes was negligible.

Lactate biosensors exhibited a sensitivity of 140.4 ± 113.5 μA mM^{-1} cm^{-2} (n=11), which was satisfactory compared to previously reported bioprobes, with an average sensitivity in the 50–400 μA mM^{-1} cm^{-2} range, reported for planar and microwire-based biosensors (Burmeister et al., 2005; Lamas-Ardisana et al., 2014; Romero et al., 2010; Tian et al., 2010). Glucose biosensors exhibited a sensitivity of 44.8 ± 37.4 μA mM^{-1} cm^{-2} (n=9) for glucose, that was comparable to glucose biosensors previously described in the literature that had a sensitivity range of 1–100 μA mM^{-1} cm^{-2} (Kang et al., 2009; McMahon et al., 2005; Tan et al., 2010; Vasylieva et al., 2011). Glucose and lactate detection was reproducible, as shown in duplicate experiments showing that the step in oxidation current recorded in response to the second injection was 100.7 ± 16.1% of the first one for glucose (n=14) and 97.0 ± 19.0% for lactate (n=8).

The brain basal glucose and lactate concentrations are expected to be in the mM range (Fellows et al., 2006; Netchiporouk et al., 1996; Ronne-Engström et al., 1995; Silver and Erecińska, 1994; Vasylieva et al., 2011; Demestre et al., 1997; Eklund et al., 1991; Harada et al., 1993, 1992). Therefore, it appeared important to obtain biosensors with a linear range extending up to 0.5–2.5 mM lactate and glucose concentrations. To obtain such a linear response of glucose and lactate biosensors, we deposited an additional top membrane of polyurethane. This membrane creates a diffusion barrier and decreases the flux of substrate to the enzymatic layer deposited on the biosensor surface. As a result, the concentration of substrate that effectively reaches the enzyme layer entrapped beneath the polyurethane membrane is lower than the actual concentration in the bath, resulting in an extended linear response range (Schuvailo et al., 2006). In our hands 3–6 layers deposited from polyurethane solution (2–3% in THF) by dip coating were sufficient to obtain a linear range (see Supplementary data Fig. SD4) extending up to 1.5–3 mM of lactate. We should note, however, that this extension is often obtained at the expense of a decreased sensitivity that is induced not only by the presence of the diffusive polyurethane layer, but also probably by the presence of THF in the polyurethane solution that could partially inactivate the enzyme.

3.3. Validation of multi-sensing probe in the brain of the anesthetized rats

To obtain an *in vivo* proof of concept we tested our multi-sensing biosensor in the brain of anesthetized rats. The three-sensor probe was implanted in the somatosensory/motor cortex. Fig. 4A shows a photograph of the rat with the implanted multi-sensor micro-probe. It visualizes the benefit of the multi-sensing probe, having only one site of implantation instead of three independent biosensors. Thus, less brain damage occurs when the multi-electrode probe is used *in vivo*. Fig. 4D illustrates an *in vivo* recording with our biosensor: glucose (red line), lactate (green line) and the control electrode (black line). In the initial portion of the experiment (first 30 min), the oxidation currents recorded by the glucose and lactate biosensors were substantially higher than those recorded by the control electrode. The difference in current between the glucose or lactate electrode and the control one divided by the sensitivity of each biosensor yielded basal extracellular glucose and lactate concentrations of 1.2 ± 0.3 mM (n=5) and 0.35 ± 0.13 mM (n=5) respectively. This is consistent with findings from studies of *in vivo* brain glucose and lactate

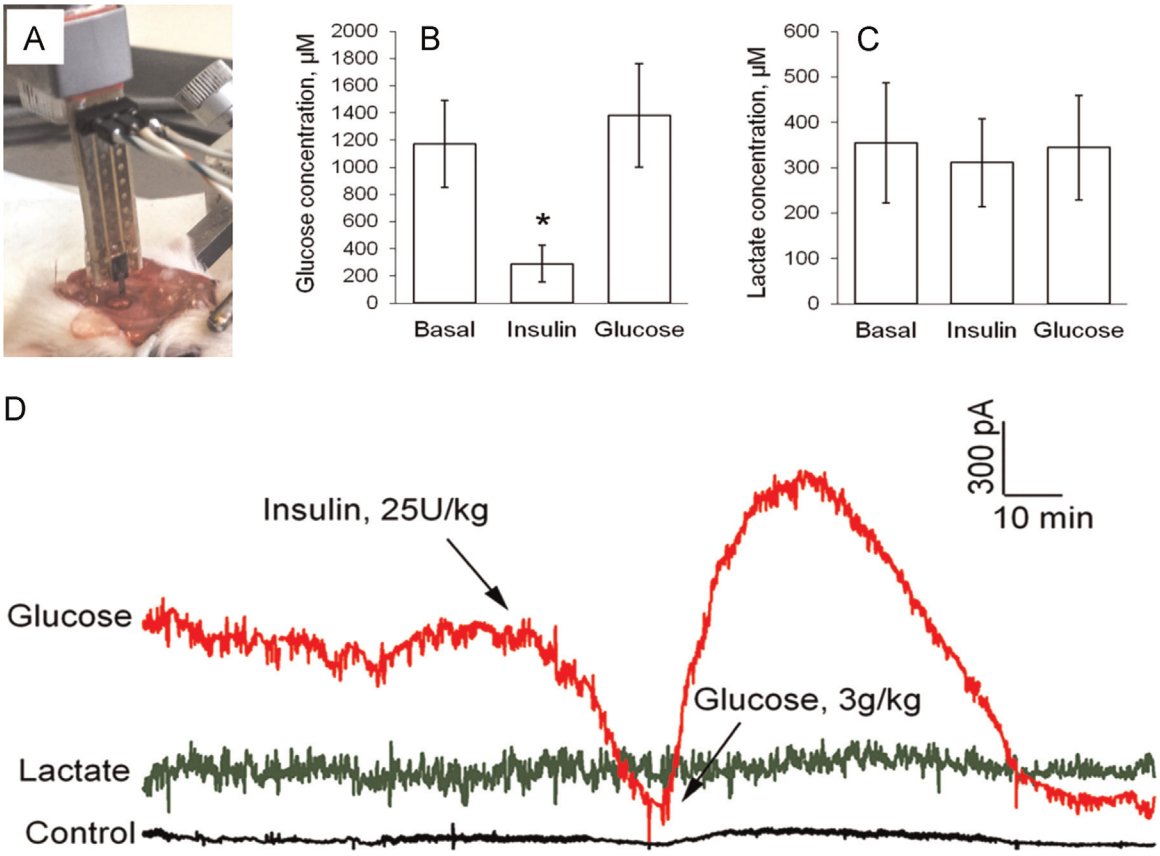

Fig. 4. *In vivo* monitoring of glucose and lactate. (A) Single-penetration probe in the cortex of anesthetized rat. Glucose (A) and lactate (C) concentrations for $n=6$ estimated before and 1 h after insulin administration and at the peak of glucose rebound. (B) Extracellular glucose decreased after insulin administration (25 U/kg); and increased following subsequent injection of glucose solution (3 g/kg). Lactate sensor response was not affected by the glucose concentration variations. (For interpretation of the references to color in this figure, the reader is referred to the web version of this article.)

monitoring with other types of biosensors (Leybaert, 2005; Lin et al., 2007; Netchiporouk et al., 1996). One of the most accurate methods to determine the basal concentration of a molecule in the brain interstitial fluid is the no-net-flux microdialysis method. It has been implemented to quantify glucose and lactate basal levels between 1 and 1.5 mM (Krebs-Kraft et al., 2009; Rex et al., 2009) and 346 μM (Demestre et al., 1997) respectively, which were very close to our estimates. By comparison, different types of enzyme biosensors provided more widespread glucose concentration estimates: 500 μM, (Calia et al., 2009); 1.3 mM (Cordeiro et al., 2015); 2.6 mM (Hu and Wilson, 2002). Lactate basal extracellular concentration was also widespread, with quantifications up to 1.6 mM (Cordeiro et al., 2015). The reasons for such discrepancies between biosensor studies are still unclear. It is possible that different biosensor architectures and sizes can significantly impact the homeostasis of the brain parenchyma, and therefore, the basal concentrations of glucose and lactate. In this regard, it is likely that smaller biosensor devices will yield more accurate concentration estimates. The *in vivo* experiments typically lasted about 3–5 h, and about 75% of our biosensors had sensitivity within $\pm 40\%$ of their initial value indicating that they were stable *in vivo*. In these biosensors, the sensitivity at the end of the *in vivo* experiment was $107 \pm 24\%$ and $84 \pm 22\%$ of its initial value ($n=6$) for glucose and lactate respectively. They also showed a sensitivity to serotonin less than 1.2 μA mM^{-1} cm^{-2} (*i.e.* $<1\%$ of the glucose, or lactate signal).

Injection of insulin (25 U/kg body weight intraperitoneally) induced a steady decrease in oxidation current from the glucose biosensor, but not from the control electrode and the lactate biosensor. Delayed injection of glucose (3 g/kg) after insulin administration quickly raised the brain glucose signal above its original value (Fig. 4D). The extracellular brain glucose concentration after insulin injection was 0.29 ± 0.13 mM ($n=6$), and the concentration rose to 1.4 ± 0.4 mM ($n=6$) after glucose administration (Fig. 4B). The concentration of extracellular lactate remained unchanged during manipulations with physiological glucose. The lactate concentrations after insulin injection and subsequent glucose administration were estimated at 0.31 ± 0.97 mM and 0.34 ± 0.12 mM ($n=6$), respectively (Fig. 4C). The effects of insulin and subsequent glucose administration are well documented (Netchiporouk et al., 1996) and are often used in validation of new tools for glucose monitoring (Lowry et al., 1998; Steil et al., 2005; Vasylieva et al., 2011; Wei et al., 2014). To our knowledge, there is no consensual pharmacological treatment that could reliably change lactate levels without impacting glucose extracellular concentrations. Therefore, we did not attempt to setup a symmetrical experiment in which lactate levels would change independently of glucose.

We should note that the extent to which our biosensor probes could injure the brain parenchyma is currently unknown. It is therefore possible that some of the lactate detected in the extracellular space could come from the bloodstream or be impacted by the presence of injured cells at the vicinity of the electrode. However, our silicon microneedle has a cross section of only 50×100 μm^2, which is smaller than most microfabricated enzymatic biosensors systems present in the literature. For example, (Weltin et al., 2014) described a polymer-based microsensor with a cross section of 100×500 μm^2 to be compared to a cross-section of 120×150 μm^2 for the microneedle designed by Wassum et al. (2008), or 120×125 μm^2 in Burmeister et al. (2000). Therefore,

the possible lesions to the brain parenchyma and the contribution of blood lactate and glucose to our measurements should be minimal with our probe.

Glucose is a main nutrient in the brain, while lactate is formed from glucose in an actively glycolyzing system under anaerobic conditions and so glucose and lactate monitoring is of interest in metabolic disorders including cerebral ischemia. A number of studies in rats and human subjects demonstrated that increasing the blood concentration of glucose does not affect extracellular lactate levels (Abi-Saab et al., 2002; Yao et al., 2004). Our results obtained with the multi-electrode micro-probes in this study are in agreement with this previously reported data. We should note, however, that a recent study by Cordeiro et al. (2015) showed a decrease in lactate levels in response to both insulin and glucose injections. The causes of this apparent discrepancy are still unclear, and could be related to the different geometry of the biosensor systems, and the number of brain penetrations in the two studies.

Extending previous studies, our multi-sensing probes allowed real time monitoring of extracellular lactate concentration in close proximity and simultaneously with glucose using a single bioprobe at one implantation site. This is a significant improvement over previous studies because a single implantation site is less damaging to brain tissue making measurements closer to physiological conditions. In contrast, large microdialysis probes with diameter of 250–300 μm were used in previously reported work for sampling of the extracellular milieu followed by delayed analysis (Abi-Saab et al., 2002). The use of wire-based single-sensing micro-biosensors would require implantation of three electrodes, one for glucose, another for lactate and the third one for controlling non-specific currents, resulting in increased damage to the brain. An additional challenge with single-sensing biosensors is the placement of all three electrodes at close proximity to one another. This requires high-precision manipulation of the biosensors, taking highly precise stereotaxic coordinates and a complex arrangement of biosensors near the site of implantation. Our multi-sensing probes overcome this problem by placing all electrodes on the same probe shaft and controlling overall geometry of the device and its design at the microfabrication step.

Additionally, the control electrode placed between the glucose and lactate biosensors detected only slight current variations following glucose modulation in the brain, indicating that cross-talk between the electrodes was negligible. Therefore, these experiments confirmed the concept of independent simultaneous *in vivo* glucose and lactate monitoring. Hence, our monitoring tool can be applied for more complex neurochemical studies, aiming to understand the metabolic regulation of energy substrates in the brain.

4. Conclusions

We report a novel architecture suitable for parallel neurochemical sensing with low cross-talk based on SU8 patterning and silicon micromachining. Three-electrodes silicon/SU8 implantable micro-needle have been successfully fabricated using MEMS-technology. With SU8-photoresist we create the insulating layer and the electrode micro-wells in a single step decreasing considerably the process-flow complexity. Using a precise local deposition technique enzymes have been grafted onto the Pt electrodes. The enzyme volume and localization was controlled by adjusting the SU8 thickness which was a key step for the successful fabrication of the sensors.

The selected sensors were tested using standard solutions *in vitro* by alternating injections of glucose and lactate. The *in vitro* experiments indicated reliable independent responses of the three-electrode micro-needle sensors and the absence of significant cross-talk. Finally the *in vivo* rat brain recordings demonstrated the concept of independent simultaneous monitoring of extracellular glucose and lactate, by modifying glucose levels without impacting lactate. Compared to previously reported single-sensing microelectrodes or microdialysis probes, we demonstrated the usefulness of the biosensors for localized, simultaneous and real time monitoring of glucose and lactate in the extracellular milieu with minimal damage to the brain tissue. This real time parallel monitoring tool will be valuable for complex neurochemical studies, including the monitoring of cerebral metabolism in the healthy or injured brain.

Acknowledgements

This study was supported by the Institut de Nanotechnologies de Lyon, CNRS UMR5270, INSA de Lyon, the Lyon Neuroscience Research Center (Inserm U1028, CNRS UMR5292, team WAKING), SFR Santé Lyon Est and Université Claude Bernard Lyon I, the French RENATECH network and by grants ANR-09-BLAN-0063 Neurosense. Natalia Vasylieva is recipient of Ph.D. fellowship from the French Ministry of Education and Research. Microfabrication was performed in Nanolyon and PTA facilities. Philippe Girard, Irene Pheng, Stephane Litaudon, Anne Meiller and Quentin Chalvet provided valuable technical assistance in probe fabrication and sensor validation.

Appendix A. Supplementary information

Supplementary data associated with this article can be found in the online version at http://dx.doi.org/10.1016/j.bios.2015.05.004.

References

Abi-Saab, W.M., Maggs, D.G., Jones, T., Jacob, R., Srihari, V., Thompson, J., Kerr, D., Leone, P., Krystal, J.H., Spencer, D.D., During, M.J., Sherwin, R.S., 2002. J. Cereb. Blood Flow Metab. 22, 271–279.
Bellander, B.-M., Cantais, E., Enblad, P., Hutchinson, P., Nordström, C.-H., Robertson, C., Sahuquillo, J., Smith, M., Stocchetti, N., Ungerstedt, U., Unterberg, A., Olsen, N.V., 2004. Intens. Care Med. 30, 2166–2169.
Bruno, J.P., Gash, C., Martin, B., Zmarowski, A., Pomerleau, F., Burmeister, J., Huettl, P., Gerhardt, G.A., 2006. Eur. J. Neurosci. 24, 2749–2757.
Burmeister, J.J., Gerhardt, G.A., 2003. TrAC–Trends Anal. Chem. 22, 498–502.
Burmeister, J.J., Moxon, K., Gerhardt, G.A., 2000. Anal. Chem. 72, 187–192.
Burmeister, J.J., Palmer, M., Gerhardt, G.A., 2005. Biosens. Bioelectron. 20, 1772–1779.
Burmeister, J.J., Pomerleau, F., Huettl, P., Gash, C.R., Werner, C.E., Bruno, J.P., Gerhardt, G.A., 2008. Biosens. Bioelectron. 23, 1382–1389.
Buzsáki, G., 2004. Nat. Neurosci. 7, 446–451.
Calia, G., Rocchitta, G., Migheli, R., Puggioni, G., Spissu, Y., Bazzu, G., Mazzarello, V., Lowry, J.P., O'Neill, R.D., Desole, M.S., Serra, P.A., 2009. Sensors 9, 2511–2523.
Cordeiro, C.A., de Vries, M.G., Ngabi, W., Oomen, P.E., Cremers, T.I.F.H., Westerink, B. H.C., 2015. Biosens. Bioelectron. 67, 677–686.
Dale, N., Hatz, S., Tian, F., Llaudet, E., 2005. Trends Biotechnol. 23, 420–428.
Demestre, M., Boutelle, M., Fillenz, M., 1997. J. Physiol. 499 (Pt 3), 825–832.
Eklund, T., Wahlberg, J., Ungerstedt, U., Hillered, L., 1991. IActa Physiol. Scand. 143, 279–286.
Fellows, L.K., Boutelle, M.G., Fillenz, M., 2006. J. Neurochem. 59, 2141–2147.
Frey, O., Holtzman, T., McNamara, R.M., Theobald, D.E.H., van der Wal, P.D., de Rooij, N.F., Dalley, J.W., Koudelka-Hep, M., 2010. Biosens. Bioelectron. 26, 477–484.
HajjHassan, M., Chodavarapu, V., Musallam, S., 2008. Sensors 8, 6704–6726.
Harada, M., Okuda, C., Sawa, T., Murakami, T., 1992. Anesthesiology 77, 728–734.
Harada, M., Sawa, T., Okuda, C., Matsuda, T., Tanaka, Y., 1993. Horm. Metab. Res. 25, 560–563.
Hu, Y., Wilson, G.S., 2002. J. Neurochem. 68, 1745–1752.
Kang, X., Wang, J., Wu, H., Aksay, I.A., Liu, J., Lin, Y., 2009. Biosens. Bioelectron. 25, 901–905.
Kipke, D.R., Shain, W., Buzsáki, G., Fetz, E., Henderson, J.M., Hetke, J.F., Schalk, G., 2008. J. Neurosci. 28, 11830–11838.
Kotzar, G., Freas, M., Abel, P., Fleischman, A., Roy, S., Zorman, C., Moran, J.M., Melzak, J., 2002. Biomaterials 23, 2737–2750.
Krebs-Kraft, D.L., Rauw, G., Baker, G.B., Parent, M.B., 2009. Eur. J. Pharmacol. 611,

44–52.
Lamas-Ardisana, P.J., Loaiza, O.A., Añorga, L., Jubete, E., Borghei, M., Ruiz, V., Ochoteco, E., Cabañero, G., Grande, H.J., 2014. Biosens. Bioelectron. 56, 345–351.
Leybaert, L., 2005. J. Cereb. Blood Flow Metab. 25, 2–16.
Lin, Y., Liu, K., Yu, P., Xiang, L., Li, X., Mao, L., 2007. Anal. Chem. 79, 9577–9583.
Lowry, J.P., Miele, M., O'Neill, R.D., Boutelle, M.G., Fillenz, M., 1998. J. Neurosci. Methods 79, 65–74.
McMahon, C.P., Killoran, S.J., O'Neill, R.D., 2005. J. Electroanal. Chem. 580, 193–202.
Moser, I., 2002. Biosens. Bioelectron. 17, 297–302.
Navarro, X., Krueger, T.B., Lago, N., Micera, S., Stieglitz, T., Dario, P., 2005. J. Peripher. Nerv. Syst. 10, 229–258.
Netchiporouk, L.I., Shram, N.F., Jaffrezic-Renault, N., Martelet, C., Cespuglio, R., 1996. Anal. Chem.
Palmisano, F., Rizzi, R., Centonze, D., Zambonin, P.G., 2000. Biosens. Bioelectron. 15, 531–539.
Pernot, P., Mothet, J.-P., Schuvailo, O., Soldatkin, A., Pollegioni, L., Pilone, M., Adeline, M.-T., Cespuglio, R., Marinesco, S., 2008. Anal. Chem. 80, 1589–1597.
Quinto, M., Palmisano, F., Koudelka-Hep, M., 2001. Analyst 126, 1068–1072, j.
Rex, A., Bert, B., Fink, H., Voigt, J.-P., 2009. Physiol. Behav. 98, 467–473.
Romero, M.R., Ahumada, F., Garay, F., Baruzzi, A.M., 2010. Anal. Chem. 82, 5568–5572.
Ronne-Engström, E., Carlson, H., Liu, Y., Ungerstedt, U., Hillered, L., 1995. J. Neurochem. 65, 257–262.
Ruther, P., Aarts, A., Frey, O., Herwik, S., Kisban, S., Seidl, K., Spieth, S., Schumacher, A., Koudelka-hep, M., Paul, O., Stieglitz, T., Zengerle, R., Neves, H., 2008. Neuron 53, 238–240.
Rutherford, E.C., Pomerleau, F., Huettl, P., Strömberg, I., Gerhardt, G.A., 2007. J. Neurochem. 102, 712–722.
Schuvailo, O.M., Soldatkin, O.O., Lefebvre, A., Cespuglio, R., Soldatkin, A.P., 2006. Anal. Chim. Acta 573-574, 110–116.
Silver, I.A., Erecińska, M., 1994. J. Neurosci. 14, 5068–5076.
Steil, G.M., Rebrin, K., Hariri, F., Jinagonda, S., Tadros, S., Darwin, C., Saad, M.F., 2005. Diabetologia 48, 1833–1840.
Suzuki, M., Akaguma, H., 2000. Sens. Actuators B: Chem. 64, 136–141.
Tan, Y., Deng, W., Chen, C., Xie, Q., Lei, L., Li, Y., Fang, Z., Ma, M., Chen, J., Yao, S., 2010. Biosens. Bioelectron. 25, 2644–2650.
Tian, F., Wu, W., Broderick, M., Vamvakaki, V., Chaniotakis, N., Dale, N., 2010. Biosens. Bioelectron. 25, 2408–2413.
Vasylieva, N., Barnych, B., Meiller, A., Maucler, C., Pollegioni, L., Lin, J.-S., Barbier, D., Marinesco, S., 2011. Biosens. Bioelectron. 26, 3993–4000.
Vasylieva, N., Maucler, C., Meiller, A., Viscogliosi, H., Lieutaud, T., Barbier, D., Marinesco, S., 2013. Anal. Chem. 85, 2507–2515.
Wassum, K.M., Tolosa, V.M., Tseng, T.C., Balleine, B.W., Monbouquette, H.G., Maidment, N.T., 2012. J. Neurosci. 32, 2734–2746.
Wassum, K.M., Tolosa, V.M., Wang, J., Walker, E., Monbouquette, H.G., Maidment, N. T., 2008. Sensors 8, 5023–5036.
Wei, W., Song, Y., Shi, W., Lin, N., Jiang, T., Cai, X., 2014. Biosens. Bioelectron. 55, 66–71.
Weltin, A., Kieninger, J., Enderle, B., Gellner, A.-K., Fritsch, B., Urban, G.A., 2014. Biosens. Bioelectron. 61, 192–199.
Yao, T., Yano, T., Nishino, H., 2004. Anal. Chim. Acta 510, 53–59.